ACS OMEGA

Open Access

This article is licensed under CC-BY 4.0

http://pubs.acs.org/journal/acsodf

Article

Molecular Engineering of Sarcosine Oxidase and Horseradish Peroxidase: Impact of Lysine Accessibility on Covalent Bioconjugation and Bioelectrocatalysis

Kamilė Ratkevičiūtė, Simonas Grybas, Ondrej Šedo, Zbyněk Zdráhal, Lidija Tetianec, and Gintautas Bagdžiūnas*

Cite This: https://doi.org/10.1021/acsomega.6c04756

Read Online

ACCESS | Metrics & More | Article Recommendations | Supporting Information

ABSTRACT: Sarcosine has emerged as a critical biomarker for the early diagnosis of prostate cancer, necessitating the development of highly sensitive and simplified electrochemical detection methods. While the bioconjugation of enzymes offers a pathway toward enhanced bioelectronic performance, biosensors based on bioconjugated sarcosine oxidase remain largely unexplored. In this study, we used a synthesized redox mediator, *N*-(ferrocenylmethyl)-6-aminohexanoic acid, featuring an extended spacer arm designed to decrease the tunneling distance between the enzyme cofactor and the electrode surface. Sarcosine oxidase and horseradish peroxidase were subjected to bioconjugation via carbodiimide-mediated coupling. The resulting bioconjugates were characterized by cyclic voltammetry, diffusion-kinetic analysis, and high-resolution mass spectrometry following tryptic and peptic digestion. Furthermore, an *in silico* structural analysis was employed to correlate lysine solvent-accessible surface area with conjugation efficiency. Based on these bioconjugates, a sarcosine biosensor was constructed and tested using human serum as real samples.

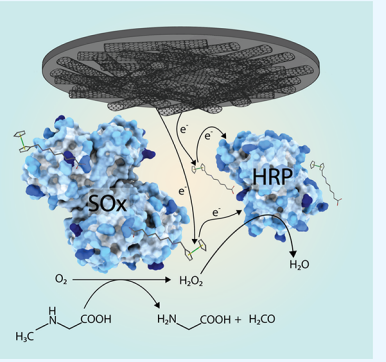

1. INTRODUCTION

Sarcosine (*N*-methylglycine) is a natural amino acid intermediate in the synthesis and degradation of glycine, found throughout human muscle and body tissues. Recently, sarcosine has emerged as a critical potential biomarker for prostate cancer.[1] Elevated concentrations in biological fluids are associated not only with prostate and colorectal cancers but also with Alzheimer's disease, dementia, stomach cancer, and sarcosinemia. Consequently, the quantitative determination of sarcosine is of paramount importance in clinical chemistry and in the food and fermentation industries.[2]

Current sarcosine detection primarily relies on enzymatic colorimetric or fluorometric assays and chromatography−mass spectrometry.[3,4] However, enzyme-based electrochemical biosensors offer a simpler, more portable alternative. Electrochemical biosensors are categorized into three generations based on their electron-transfer mechanisms. First-generation biosensors monitor the consumption of molecular oxygen or the production of hydrogen peroxide.[5] Second-generation biosensors employ a redox mediator to facilitate electron transfer between the enzyme cofactor and the electrode. Third-generation biosensors aim for direct electron transfer (DET) between the oxidase and the electrode, eliminating the need for mediators. To bridge the gap between these generations, Heller[6] and Sode,[7] with colleagues, introduced the "2.5th generation" principle. This approach uses "quasi-DET" enzymes, in which a mediator is bioconjugated directly to the enzyme.

Understanding charge carrier transport (electrons and holes) through proteins is fundamental to both natural processes, such as photosynthesis and respiration, and the development of artificial biosystems.[8−10] In the third-generation biosensors, redox-active amino acid residues (e.g., tryptophan and tyrosine) facilitate a proton-coupled carrier transfer.[11] We have previously argued that charge transport in these proteins is more accurately described as "hole hopping" rather than electron conduction, because long-range electron transport is physically restricted to charge tunneling.[12] Our recent studies demonstrated that internal tryptophan residues in glucose oxidase from *Aspergillus niger* are essential for hole hopping to the cofactor. Furthermore, we identified that the "bottleneck" stage is the hole transfer between the attached mediator and the electrode surface. By leveraging these principles, we successfully transformed bioconjugated enzymes into semiconductors while preserving their biocatalytic activity.[13]

Received: April 27, 2026
Revised: October 9, 2026
Accepted: October 12, 2026

ACS Publications

© XXXX The Authors. Published by American Chemical Society

Downloaded from pubs.acs.org/acsodf/article-pdf/doi/10.1021/acsomega.6c04756/6907591 2/acsomega.6c04756.pdf by guest on 04 November 2026

Table 1. The Biocatalytic, Electrochemical Properties, and the Bioconjugation Position of FcAHA-SOx and FcAHA-HRP[a]

Bioconjugate	Bioactivity of native/product, U mg^{-1}	Anodic electrochemical potential ($E_{1/2}$), V vs Ag/AgCl	Diffusion coefficient (D), cm^2 s	Bioconjugation position (modification degree)
FcAHA-SOx	1.8/0.27	0.337 ± 0.008	6.1×10^{-7}	Lys365 (2%)
FcAHA-HRP	99/92	0.340 ± 0.010	5.4×10^{-6}	Not detected

[a]The D value of free FcAHA was estimated to be 3.9×10^{-6} cm^2 s^{-1}.

While glucose oxidase has been extensively engineered for quasi-DET applications,[14,15] similar bioconjugation has been applied to glucose dehydrogenase, NAD(P)-dependent dehydrogenases, and glutamate oxidase.[16−20] However, sarcosine oxidase (SOx) remains underutilized in this context. SOx is a flavoenzyme that catalyzes the oxidative demethylation of sarcosine into glycine, formaldehyde, and hydrogen peroxide.[20] Currently, SOx-based electrochemical biosensors are limited to first- or second-generation designs; no bioconjugated, quasi-DET-based SOx biosensors have been reported in the literature.

In parallel, horseradish peroxidase (HRP) is widely used in biotechnology for its rapid catalysis of hydrogen peroxide reduction.[21] The covalent bioconjugation of HRP to various moieties is a standard technique for enhancing sensitivity and specificity.[22,23] Notably, Carolan et al. demonstrated that covalent attachment of ferrocene to HRP glycans creates an efficient mediation pathway between the enzyme cofactor and the electrode.[24]

In this work, SOx and HRP were bioconjugated with a ferrocene-based electrochemically active functional group with an extended aliphatic chain. This modification was designed to enhance the electrochemical biosensor performance compared to the corresponding native enzymes. The resulting bioconjugates were rigorously characterized to confirm their structural and electrochemical properties. To identify the specific amino acid residues of SOx that were functionalized, enzymatic digestion followed by high-resolution mass spectrometry was employed. The analytical performance and clinical utility of the bioconjugated biosensor for monitoring sarcosine levels were validated using human blood serum samples.

2. MATERIALS AND METHODS

Materials and detailed experimental procedures regarding the chemical synthesis, bioconjugation protocols, and spectral characterization are provided in the Supporting Information. Additionally, comprehensive results from mass spectrometry, biocatalytic assays, and theoretical structural investigations are included.

3. RESULTS AND DISCUSSION

Ferrocene (Fc) is widely used as an electrochemically active moiety in enzymatic bioconjugation to facilitate charge-carrier transport between the redox-active cofactor and the electrode surface, as well as a redox mediator in the electrolyte.[25] Our previous studies identified that the rate-limiting step in this process is charge tunneling between the enzyme surface and the electrode.[13] Specifically, when ferrocene carboxylic acid (FcCOOH) was conjugated to glucose oxidase, the resulting charge transport was too slow to support high-performance glucose biosensing.[26] Based on these theoretical and experimental insights, we hypothesize that increasing the length of the spacer arm between the Fc group and the enzyme surface will decrease the effective tunneling distance to the electrode. By extending the reach of the redox group, the probability of charge tunneling between the functionalized enzyme and the electrode surface is expected to increase significantly. Using the optimized structures of FcCOOH and *N*-(ferrocenylmethyl)-6-aminohexanoic acid (FcAHA) by density function theory (DFT), in which an amide bond replaced the carboxylic acid group, the distances between the Fe atom and the amide nitrogen were measured to be 4 Å and 13 Å, respectively.

To test this hypothesis, we synthesized FcAHA via the reductive amination of ferrocenecarboxaldehyde with 6-aminohexanoic acid (Figure S1). The resulting FcAHA compound was purified and characterized (see Supporting Information for details). For the preparation of the bioconjugates, we targeted the functionalization of primary amine groups (Lys residues) on the surfaces of SOx and HRP via amide bond formation. The carboxylic acid group of FcAHA was activated using 1-ethyl-3-(3-(dimethylamino)propyl) carbodiimide (EDC) and *N*-hydroxysuccinimide (NHS) in potassium phosphate buffer (PPB, 50 mM, pH 7.0). The native enzymes were then introduced to the activated homogeneous mixture and left at 4 °C overnight. Following the chemical reaction, protein aggregates and insoluble byproducts were removed via centrifugation. The resulting clear supernatant was purified by dialysis against PPB (pH 7.0) to yield the final FcAHA-HRP and FcAHA-SOx bioconjugates.

Following the bioconjugation, the specific biocatalytic activities of the native enzymes and their corresponding bioconjugates (FcAHA-HRP and FcAHA-SOx) were determined. The measurements were performed using the initial rate method, employing *o*-dianisidine as a chromogenic substrate. To calculate specific activity, the concentrations of the modified enzymes were determined spectrophotometrically. The biocatalytic performance of the functionalized enzymes was benchmarked against their native counterparts, as summarized in Table 1. For HRP, the modification was well-tolerated, with only a 7% decrease in specific activity, indicating that the spacer arm and ferrocene moiety did not significantly disrupt the active site or protein folding. In contrast, the specific activity of SOx decreased substantially following the bioconjugation. The FcAHA-SOx bioconjugate retained only 15% of the native activity of SOx.

To confirm the attachment of the FcAHA moiety to the enzymes, the absorption spectra of the native enzymes and the FcAHA-HRP and FcAHA-SOx bioconjugates were compared. However, UV−vis spectroscopy provided no discernible evidence of the bioconjugation (Figure S1). The calculated ratios of mediator and protein molecules in the modified enzymes were 1.9 ± 0.3 for HRP and 3.3 ± 0.9 for SOx, respectively. However, estimates of the conjugation degree based on these absorption spectra lacked the necessary sensitivity for reliable quantification (see the Supporting Information, Figure S2). Consequently, the electrochemical properties of the free FcAHA redox mediator and its bioconjugates were studied by cyclic voltammetry (CV), with potential sweeps from 0 to 0.6 V versus Ag/AgCl. Glassy

Downloaded from pubs.acs.org/acsodf/article-pdf/doi/10.1021/acsomega.6c04756/6907591/2/acsomega.6c04756.pdf by guest on 04 November 2026

https://doi.org/10.1021/acsomega.6c04756
ACS Omega XXXX, XXX, XXX−XXX

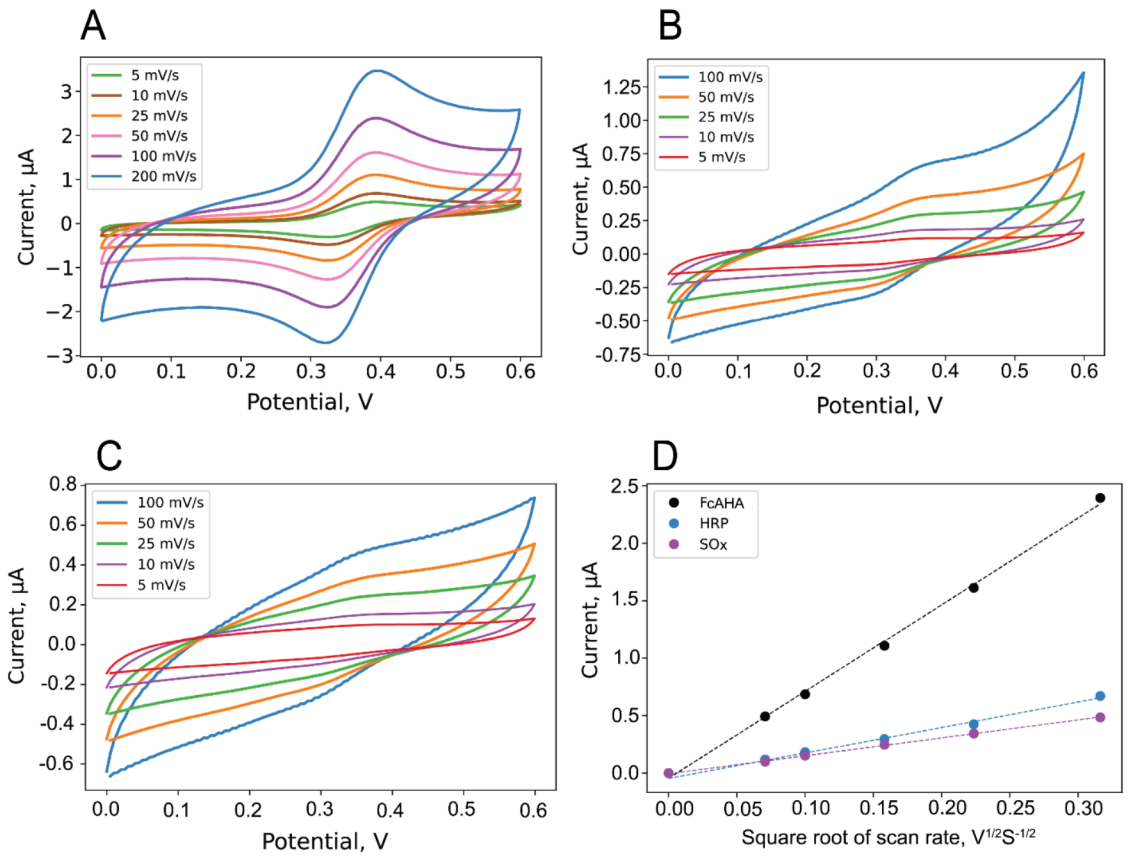

Figure 1. Characterization of the modified electrodes via varying scan rates. Cyclic voltammograms recorded at different scan rates (from 5 to 100 mV s^{-1}) for: (A) free FcAHA (c = 200 μM); (B) HRP (c = 50 μM); (C) FcAHA-SOx (c = 104 μM); (D) the linear regression plots representing the relationship between the peak current and the square root of the scan rate for the mediator (black). HRP (blue), and SOx (purple). The linear correlation observed in all cases (R^2 > 0.99) indicates that the redox processes on the modified electrode surfaces are diffusion-controlled. All measurements were conducted at room temperature in the PPB pH 7.0 solution containing 100 mM KCl.

carbon disk electrodes were used to investigate the electrochemical properties, while graphite disk electrodes, prepared from graphite rods by insulation of their cylindrical surface, were utilized for the construction of the biosensors. As shown in Figure 1, both the FcAHA-HRP and FcAHA-SOx solutions exhibited a reversible anodic peak at 0.34 V vs Ag/AgCl, consistent with the redox potential of the free FcAHA mediator. Given that the bioconjugates were purified via exhaustive dialysis to remove small molecules, the presence of this signal indicates that the redox group is either covalently or noncovalently associated with the enzyme surface. It should be noted that the electrochemical signals of flavin-dependent oxidases[27] or HRP[28] typically occur at significantly more negative electrode potentials; thus, the observed peaks are characteristic of the FcAHA moiety.

To further elucidate the nature of the FcAHA association, the scan rate (v) was varied from 5 to 100 mV s^{-1}. In all cases, a linear correlation was observed between the oxidation peak current (I_p) and the square root of the scan rate ($v^{1/2}$), confirming that the electrochemical processes are diffusion-controlled (Figure 1d). The diffusion coefficients (D) were calculated using the Randles-Ševčík equation (eq S1). The calculated D values are summarized in Table 1. For the FcAHA-HRP bioconjugate, the diffusion coefficient remained comparable to that of the free FcAHA mediator. It suggests that the electrochemical signal in the FcAHA-HRP sample likely originates from a redox mediator noncovalently adsorbed to the protein surface rather than covalently bioconjugated. Conversely, the diffusion coefficient of 6.1 × 10^{-7} cm^2 s^{-1} for the FcAHA-SOx bioconjugate was significantly lower, aligning with the expected diffusion rates for globular proteins. While small-molecule redox mediators typically exhibit D values in the range of 10^{-5} to 10^{-6} cm^2 s^{-1}, proteins of this molecular weight (in the range of 45−160 kDa) generally possess diffusion coefficients an order of magnitude lower, ranging from 4.0 × 10^{-7} to 8.0 × 10^{-7} cm^2 s^{-1} in the aqueous solution.[29] This substantial reduction in the diffusion coefficient for the FcAHA-SOx bioconjugate provides robust evidence that the FcAHA moiety is successfully attached to the enzyme.

To determine the specific conjugation sites, the FcAHA-HRP and FcAHA-SOx bioconjugates were subjected to enzymatic proteolysis using pepsin and trypsin, followed by analysis via high-resolution mass spectrometry (HRMS). For the FcAHA-SOx bioconjugate, the results varied significantly depending on the protease employed. The tryptic digestion successfully revealed functionalization at Lys365 (Table 1), confirming covalent attachment at this specific Lys residue. However, when pepsin was used for hydrolysis, no functionalized peptide fragments were detected. This discrepancy may be attributed to specific cleavage patterns of pepsin, which can yield fragments in which the modified Lys is part of a sequence that is difficult to ionize or detect under the experimental conditions.

In contrast, no functionalization was observed for the FcAHA-HRP sample in either the tryptic or peptic digests. To

Downloaded from pubs.acs.org/acsodf/article-pdf/doi/10.1021/acsomega.6c04756/6907591 2/acsomega.6c04756.pdf by guest on 04 November 2026

https://doi.org/10.1021/acsomega.6c04756
ACS Omega XXXX, XXX, XXX−XXX

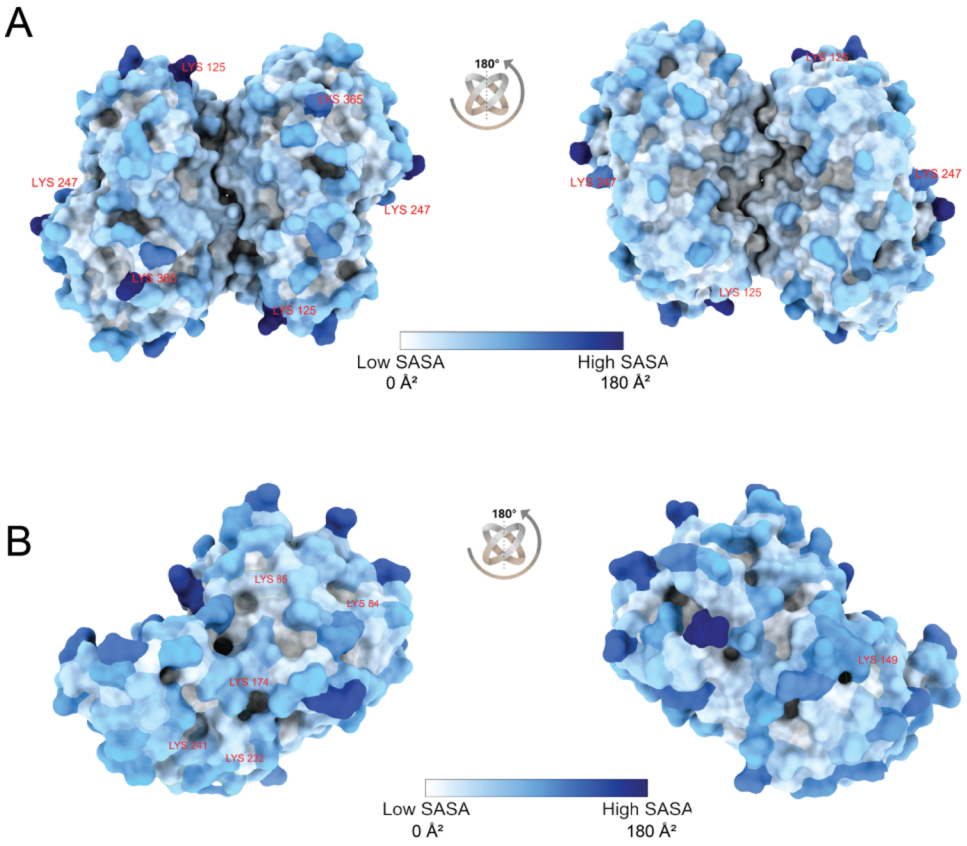

Figure 2. Solvent accessible surface area (SASA) mapping of HRP and SOx. Surface representation of (A) HRP and (B) SOx, showing two views of each protein (rotated 180°). The surfaces are color-coded by SASA value, with a gradient from white to dark blue corresponding to the accessibility scale of 0−180 A^2. The Lys residues exhibiting the highest SASA values are highlighted with a red label.

further verify this, direct mass spectrometry of the intact FcAHA-HRP protein was performed without the prior enzymatic digestion. This analysis showed no detectable increase in the molecular ion mass compared to the native enzyme (Figure S3). These findings, combined with the earlier diffusion coefficient data, confirm that the FcAHA moiety in the FcAHA-HRP sample was merely adsorbed rather than covalently bound to the scaffold of the enzyme.

To elucidate the low modification efficiency for SOx and the absence of covalent modification in HRP, we performed a comprehensive structural analysis. For every Lys residue on the surfaces of both enzymes, the solvent-accessible surface area (SASA) and the specific secondary structure elements to which it belongs were estimated. Using the Adaptive Poisson−Boltzmann Solver (APBS), we estimated pK_a values and identified potential intraenzymatic hydrogen-bonding networks involving the Lys side chains.[30] The SOx homodimer (PDB ID: 9U3D)[31] contains 21 Lys residues per monomer. Our calculations showed that the pK_a values for most of these residues exceed 10.0. Under our experimental conditions (pH 7.0), this implies that less than 0.1% of the amines are in the deprotonated, nucleophilic state required for the EDC/NHS-mediated amide bond formation. The low fraction of deprotonated lysine residues at pH 7.0 does not limit the reaction kinetics, as the formation of the covalent amide bond effectively pulls the acid−base equilibrium toward the nucleophilic species. Although seven Lys residues exhibited pK_a values below 10.0, they were either deeply buried within the protein core, part of rigid secondary structures, or stabilized by intraenzymatic hydrogen bonds (Table S1). The modified residue of Lys365 identified by HRMS Lys365 is located within a flexible coil and is not involved in intraenzymatic hydrogen bonding (Figure 2). It exhibits a high SASA of 159.1 $Å^2$ in the A chain and 147.9 $Å^2$ in the B chain of SOx, respectively. While Lys125 possesses a higher SASA, its integration into an α-helix may limit its conformational accessibility. Lys274 displays structural parameters similar to Lys365, suggesting it could be an additional potential target, though HRMS did not detect it in this study.

In contrast, the HRP structure (PDB ID: 1HCH)[32] contains only 6 Lys residues, none of which appear to be viable targets for the covalent fictionalization. The maximum SASA observed was only 80.2 $Å^2$, and most of the Lys side chains are sequestered by intraenzymatic hydrogen bonds (Table S2). Despite the lack of covalent bonding confirmed by HRMS, spectroscopic and electrochemical data (see the Supporting Information) clearly indicate the presence of the FcAHA mediator in the FcAHA-HRP sample. This discrepancy can be explained by the noncovalent adsorption of the mediator to the enzyme surface, likely driven by hydrophobic or electrostatic interactions rather than the intended amide linkage.

To investigate the bioelectrocatalytic activity of the FcAHA-SOx bioconjugate, the enzyme was immobilized onto a glassy carbon electrode (GCE). The enzyme solution was drop-casted onto the electrode surface and subsequently secured with a dialysis membrane to ensure the enzyme retention and stability at the electrode interface. CV was performed in a microcell in the presence of 10 mM sarcosine; however, Figure S4 reveals only negligible changes in current. It indicates that DET was not effective. The absence of a DET response likely

Downloaded from pubs.acs.org/acsodf/article-pdf/doi/10.1021/acsomega.6c04756/6907591/2/acsomega.6c04756.pdf by guest on 04 November 2026

https://doi.org/10.1021/acsomega.6c04756
ACS Omega XXXX, XXX, XXX−XXX

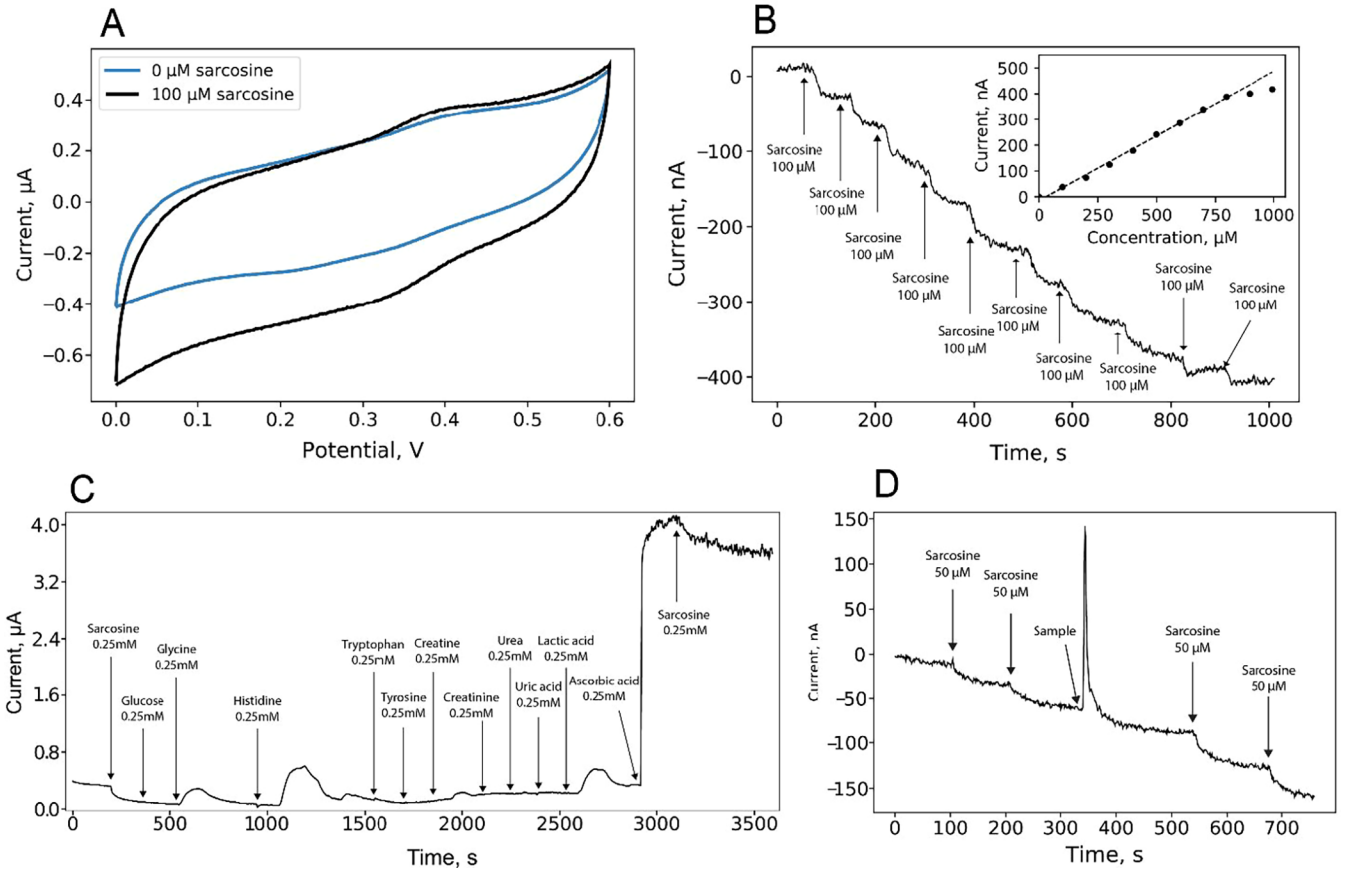

Figure 3. Electrochemical characterization of the GCE/CNT/FcAHA-HRP + FcAHA-SOx bioelectrode: (A) CVs of the bienzymatic biosensor in the absence and presence of sarcosine at a scan rate of 50 mV s^{-1}; (B) amperometric calibration curve of the biosensor upon successive additions of sarcosine (inset: steady-state current vs sarcosine concentration dependence, where the response current was determined as the net current change recorded 80−100 s postanalyte addition); (C) selectivity of the biosensor in the presence of common interfering compounds; (D) hybrid calibration curve and practical application in real sample analysis. All measurements were performed in 50 mM PPB pH 7.0 with 100 mM KCl, and the CA measurements were recorded at an applied working potential of 0.20 V vs Ag/AgCl.

stems from the low residual catalytic bioactivity of FcAHA-SOx and the insufficient density and position of the attached FcAHA mediator molecules. Consequently, we transitioned to a bienzymatic biosensor design. In the biosensor, carbon nanotubes (CNTs) were utilized to increase the electroactive surface area and maximize enzyme loading (Figure S5). To enhance sensitivity for low substrate concentrations, a GCE/CNT/FcAHA-HRP + FcAHA-SOx bioelectrode was constructed. Both bioconjugates were coimmobilized on the CNT-modified GCE and stabilized with a Nafion polymer coating. The CV analysis (Figure 3a) of this bienzymatic system identified an optimal operating potential of 0.20 V (vs Ag/AgCl). The bioelectrode was subsequently employed as an amperometric sarcosine biosensor.

Our proposed operating principle of the biosensor is based on an enzymatic cascade reaction. First, the substrate is oxidized by the immobilized SOx, generating H_2O_2 as a byproduct. Subsequently, the generated H_2O_2 reacts with HRP, converting the enzyme into its oxidized state. Because the redox mediator is covalently bioconjugated to both SOx and HRP, it acts as an efficient electron relay system as an auxiliary electron source. The analytical signal is generated when the oxidized redox mediator is electrochemically reduced back to its initial state at the electrode surface, resulting in a measurable cathodic reduction current.

Figures 3b, S6, and S7 display the amperometric titration of sarcosine, which demonstrated a linear response range up to ∼800 μM with a calculated sensitivity of 0.47 nA μM^{-1}. This upper linear limit is likely governed by the molecular oxygen-dependent nature of the bienzymatic reaction, wherein local molecular oxygen depletion limits the reaction rate at higher analyte concentrations. Although a response was observed at sarcosine concentrations below 50 μM, the data were unreliable due to system noise. The linear relationship between the current response and the sarcosine concentration was used to determine the limit of detection (LoD). Mathematically, the LoD is defined as the lowest analyte concentration that can be reliably distinguished from background noise with statistical significance, though not necessarily quantified.[33] It was calculated as three times the standard deviation of the blank divided by the slope of the calibration curve (eq S2). For this system, the LoD was determined to be 11 μM. Furthermore, the biosensor exhibited good reproducibility, yielding a relative standard deviation (RSD) of 5.8% based on five consecutive measurements of 0.25 mM sarcosine using a single device (Figure S8). The repeatability of the fabricated biosensors was evaluated across five independent electrodes, yielding RSD of 9.1%. This degree of intersensor variance indicates that, while the underlying measurement protocol is robust, the manual assembly process introduces unavoidable inconsistencies. Specifically, minor variations in the surface roughness of the

Downloaded from pubs.acs.org/acsodf/article-pdf/doi/10.1021/acsomega.6c04756/6907591/2/acsomega.6c04756.pdf by guest on 04 November 2026

https://doi.org/10.1021/acsomega.6c04756
ACS Omega XXXX, XXX, XXX−XXX

Table 2. Our Biosensor Comparison with Other Amperometric SOx-Based Sarcosine Biosensors

	Linear range, μM	Sensitivity, nA/μM	LOD, μM	RSD	Working potential, V vs Ag/AgCl	References
GCE electrode-graphene-chitosan-silver NPs-SOx	1.0−177	2.4	1	3.45%	−0.45	27
GCE electrode-Polyamic acid-SOx	0.001−0.05[a]	Not Reported	0.00004	4.6%	−0.55	34
Gold electrode-SOx nano particles	0.1−100	Not Reported	0.01	Not Reported	1	35
SOxENs/PB/SPCE	10−100	1.98	0.66	5%	0.1	36
Graphite disk electrode-CNT-FC modified HRP and SOx	50−800	0.47	11	5.8%	0.20	This work

[a]Linear range reported in logarithmic scale of concentrations.

polished graphite disk electrodes were prepared from graphite rods by insulating their cylindrical surface with heat-shrink tubing, compounded by slight differences in the manual deposition of the CNTs, enzyme-mediator conjugates, and the Nafion films, lead to localized fluctuations in both the active surface area and the mass-transport properties of each individual electrode.

The selectivity of the biosensor was evaluated by introducing potential interferents commonly found in clinical matrices, including glucose, glycine, L-histidine, L-tryptophan, L-tyrosine, creatine, creatinine, urea, uric acid, L-lactic acid, and L-ascorbic acid, at concentrations of 0.25 mM (Figure 3c). Minor transient responses were observed upon the addition of glycine, L-histidine, creatine, and L-lactic acid; however, these signals returned to the baseline shortly after injection. Among all tested species, only L-ascorbic acid produced a significant and sustained electrochemical signal, which is attributed to its direct oxidation at the electrode surface at the operating potential. To ensure that these compounds did not passivate or foul the bioelectrode surface, sarcosine was injected both before and after the addition of the interfering suite. The biosensor maintained a consistent response to both sarcosine additions, confirming that the electrode sensitivity remained unaffected by exposure to these biological compounds. Furthermore, a control electrode lacking the immobilized enzymes was evaluated under identical conditions to differentiate between direct electrochemical oxidation and enzyme-mediated interactions (Figure S9). Among the tested compounds, only L-ascorbic acid produced a significant electrochemical signal. This response is characteristic of the direct oxidation of ascorbic acid at the operating potential of 0.20 V vs Ag/AgCl. The used concentration of Nafion is theoretically sufficient to form a relatively thick protective film on the electrode surface. Nevertheless, a residual response to the addition of L-ascorbic acid was observed. This phenomenon is likely attributable to an inhomogeneous distribution of the Nafion layer across the electrode surface. Due to the inherent limitations of the drop-casting method employed for this film deposition, the evaporation dynamics can lead to a macroscopically uneven film. Consequently, these suboptimally covered regions allow the direct electrochemical oxidation of ascorbate at the exposed carbon sites. However, this structural nonuniformity did not compromise the practical utility of the biosensor, as no endogenous ascorbic acid interference was detected during the analysis of real human serum samples. Despite this sensitivity to ascorbic acid, the biosensor demonstrated high selectivity against the remaining metabolites and amino acids.

Control electrodes fabricated with native enzyme combinations (SOx + HRP) or partial bioconjugates (FcAHA-SOx + HRP) yielded significantly poorer analytical performance (Table 2, Figure S6). These comparative results confirm the synergistic benefit of incorporating both bioconjugated enzymes within the sensing layer. Specifically, the data demonstrate that noncovalently adsorbed FcAHA molecules, particularly those associated with the HRP scaffold, act as effective redox mediators within the enzyme matrix. These adsorbed species facilitate charge transfer between the biocatalytic centers and the electrode, thereby enhancing the sensitivity and overall analytical performance of the biosensor. It suggests that the sensing mechanism relies on a dual pathway: a robust covalent link in the SOx component and a highly mobile, adsorbed mediator population associated with the HRP component.

Most existing amperometric biosensors for sarcosine that use SOx exhibit excellent analytical performance, good reproducibility, low detection limits, and high sensitivity. However, these metrics often come at the expense of practical utility. For example, Li et al.[34] fabricated a biosensor capable of measuring extremely low concentrations, yet the device lacks a broad linear range. Therefore, it is restricted to a very narrow concentration window. In real-world applications, this requires highly diluting the analytes, which introduces experimental error and reduces measurement precision. While other biosensors offer decent linear ranges, they often require high working potentials, which increase their susceptibility to interference from other electroactive species in biological samples. A biosensor using Prussian blue offers a low working potential similar to ours, but it requires complex, multistep surface preparation.[36]

The analytical utility of our biosensor for clinical applications was evaluated using human serum in a 1 mL electrochemical cell. The real samples are diluted with the PPB pH 7.0 solutions. This pretreatment minimizes matrix effects while maintaining the same pH 7.0 and ionic strength used during the titration and calibration experiments, ensuring baseline consistency. To account for potential matrix effects, a hybrid standard addition approach was employed. Specifically, two standard additions of sarcosine (50 μM each) were introduced, followed by the addition of the serum sample, and concluded with two further 50 μM sarcosine additions directly into the electrochemical cell (Figure 3d). This strategy enables simultaneous calibration and quantification of the analyte within a single cell and an identical chemical microenvironment. Following each addition, the current response was recorded after ∼60 s. The unknown analyte concentration in the serum samples was calculated relative to the postsample slope of hybrid calibrations. Conducting both calibration and sample measurements within the same analytical run ensures that any baseline drift affects all signals equally, thereby minimizing systematic errors, such as electrode degradation, during analysis. This measurement was repeated three times (*n*

Downloaded from pubs.acs.org/acsodf/article-pdf/doi/10.1021/acsomega.6c04756/6907591/2/acsomega.6c04756.pdf by guest on 04 November 2026

https://doi.org/10.1021/acsomega.6c04756
ACS Omega XXXX, XXX, XXX−XXX

= 3). Since native bovine serum contains no detectable sarcosine, samples were spiked with 200 μM sarcosine to simulate pathological concentrations relevant to prostate cancer diagnostics. Upon introduction to the electrochemical cell, the human serum was diluted 4-fold.

Employing this measurement protocol, the biosensor demonstrated high accuracy with a mean recovery of 89% and an average calculated concentration of 180 ± 60 μM (n = 3, 95% CI). To assess the selectivity of the system within a complex biological environment, native human serum (unspiked) was analyzed as a control (Figure S10). The mean background current from the serum matrix was only 2 nA, approximately 88 times lower than that from the sarcosine-containing samples. These results indicate that the electrochemical interference from the serum matrix is negligible, confirming the high specificity of the GCE/CNT/FcAHA-HRP+FcAHA-SOx biosensor for the sarcosine detection in clinical matrices.

4. CONCLUSIONS

This study successfully demonstrated the development of a bienzymatic electrochemical biosensor for the detection of sarcosine, leveraging the strategic bioconjugation of sarcosine oxidase (SOx) and horseradish peroxidase (HRP). By employing a ferrocene-based redox mediator with an extended spacer arm, we addressed the challenges of charge transport in the flavoenzyme and peroxidase system. High-resolution mass spectrometry and *in silico* structural analysis confirmed that, while SOx was covalently functionalized at Lys365, HRP facilitated charge transfer primarily via noncovalent adsorption of the ferrocene-based mediator. This disparity was successfully correlated to the solvent-accessible surface area of the available lysine residues, providing a predictive framework for future enzyme engineering in bioelectronics. Although covalent modification of SOx resulted in an 85% decrease in biocatalytic activity, integrating both bioconjugates into a carbon nanotube-enhanced architecture effectively compensated for this loss. The resulting bienzymatic system operated at a low overpotential of 0.20 V (vs Ag/AgCl), exhibiting a sensitivity of 0.47 nA μM^{-1} and a clinically relevant limit of detection of 11 μM. The robustness of the biosensor was further validated by its high selectivity against common biological interferents and a good recovery rate in human serum samples. Ultimately, combining with a deep understanding of protein surface topography is a viable strategy for designing the next generation of high-performance bioconjugate-based biosensors and bioelectronic tools.

■ ASSOCIATED CONTENT

Data Availability Statement

The data supporting the findings of this study are available in the article and its Supporting Information.

Supporting Information

The Supporting Information is available free of charge at https://pubs.acs.org/doi/10.1021/acsomega.6c04756.

Materials, instrumentation, synthesis of electron transfer mediators, and enzyme-mediator bioconjugates, spectral investigations, mass spectrometry measurements, details of DFT computations, comprehensive structural analyses of SOx and HRP, enzyme immobilization, electrochemical studies, data processing, and experimental controls. The authors have cited additional references within the Supporting Information to provide further methodological context (PDF)

■ AUTHOR INFORMATION

Corresponding Author

Gintautas Bagdžiūnas − *Group of Supramolecular Analysis and Bioelectronics, Institute of Biochemistry at Life Sciences Centre, Vilnius University, LT-10257 Vilnius, Lithuania;* orcid.org/0000-0002-9924-6902; Phone: +370 5 2234393; Email: gintautas.bagdziunas@gmc.vu.lt

Authors

Kamilė Ratkevičiūtė − *Group of Supramolecular Analysis and Bioelectronics, Institute of Biochemistry at Life Sciences Centre, Vilnius University, LT-10257 Vilnius, Lithuania*

Simonas Grybas − *Group of Supramolecular Analysis and Bioelectronics, Institute of Biochemistry at Life Sciences Centre, Vilnius University, LT-10257 Vilnius, Lithuania*

Ondrej Sedo − *Central European Institute of Technology, Masaryk University, 625 00 Brno, Czech Republic*

Zbyněk Zdráhal − *Central European Institute of Technology, Masaryk University, 625 00 Brno, Czech Republic; National Centre for Biomolecular Research, Faculty of Science, Masaryk University, 625 00 Brno, Czech Republic;* orcid.org/0000-0003-3044-5548

Lidija Tetianec − *Group of Supramolecular Analysis and Bioelectronics, Institute of Biochemistry at Life Sciences Centre, Vilnius University, LT-10257 Vilnius, Lithuania*

Complete contact information is available at: https://pubs.acs.org/10.1021/acsomega.6c04756

Author Contributions

K.R., L.T., G.B.: Conceptualization. K.R., S.G., O.Š.: Methodology. L.T., K.R., S.G., O.Š.: Formal analysis. G.B., Z.Z.: Supervision. K.R., L.T., G.B.: Writing—original draft. G.B.: Writing—review and editing. All authors have given approval to the final version of the manuscript.

Notes

The authors declare no competing financial interest.

■ ACKNOWLEDGMENTS

This work was supported by the "Nanostructured Bioconjugates for Quantum Bioelectronics" project, funded by the Research Council of Lithuania (LMTLT) under agreement no. S-ITP-25-11. The authors gratefully acknowledge CIISB, Instruct-CZ Centre of the Instruct-ERIC EU consortium, for financial support regarding measurements performed at the CEITEC Proteomics Core Facility. This infrastructure is funded by the MEYS CR project LM2023042 and the European Regional Development Fund project "Innovation of Czech Infrastructure for Integrative Structural Biology" (No. CZ.02.01.01/00/23_015/0008175). Additionally, computational resources were provided by the e-INFRA CZ project (ID: 90254), supported by MEYS CR.

■ REFERENCES

(1) Cernei, N.; Heger, Z.; Gumulec, J.; Zitka, O.; Masarik, M.; Babula, P.; Eckschlager, T.; Stiborova, M.; Kizek, R.; Adam, V. Sarcosine as a Potential Prostate Cancer Biomarker—A Review. *Int. J. Mol. Sci.* **2013**, *14* (7), 13893−13908.

Downloaded from pubs.acs.org/acsodf/article-pdf/doi/10.1021/acsomega.6c04756/6907591/2/acsomega.6c04756.pdf by guest on 04 November 2026

(2) Pundir, C. S.; Deswal, R.; Yadav, P. Quantitative Analysis of Sarcosine with Special Emphasis on Biosensors: A Review. *Biomarkers* **2019**, *24* (5), 415−422, DOI: 10.1080/1354750x.2019.1615124.
(3) Burton, C.; Gamagedara, S.; Ma, Y. A Novel Enzymatic Technique for Determination of Sarcosine in Urine Samples. *Anal. Methods* **2012**, *4* (1), 141−146.
(4) Lan, J.; Xu, W.; Wan, Q.; Zhang, X.; Lin, J.; Chen, J.; Chen, J. Colorimetric Determination of Sarcosine in Urine Samples of Prostatic Carcinoma by Mimic Enzyme Palladium Nanoparticles. *Anal. Chim. Acta* **2014**, *825*, 63−68.
(5) Lukoševičius, E.; Kravčenko, J.; Mikėnaitė, G.; Markevičius, A.; Bagdžiūnas, G. Universal Platform Based on Carbon Nanotubes Functionalised with Carboxylic Acid Groups for Multi-Analyte Enzymatic Biosensing. *Biosensors* **2025**, *15* (10), No. 686, DOI: 10.3390/bios15100686.
(6) Schuhmann, W.; Ohara, T. J.; Schmidt, H. L.; Heller, A. Electron Transfer between Glucose Oxidase and Electrodes via Redox Mediators Bound with Flexible Chains to the Enzyme Surface. *J. Am. Chem. Soc.* **1991**, *113* (4), 1394−1397.
(7) Hatada, M.; Loew, N.; Inose-Takahashi, Y.; Okuda-Shimazaki, J.; Tsugawa, W.; Mulchandani, A.; Sode, K. Development of a Glucose Sensor Employing Quick and Easy Modification Method with Mediator for Altering Electron Acceptor Preference. *Bioelectrochemistry* **2018**, *121*, 185−190.
(8) Saboe, P. O.; Conte, E.; Farell, M.; Bazan, G. C.; Kumar, M. Biomimetic and Bioinspired Approaches for Wiring Enzymes to Electrode Interfaces. *Energy Environ. Sci.* **2017**, *10* (1), 14−42.
(9) Black, N. E.; Cheng, D.; Grasty, B. P.; Boucher, D. G. Artificial Enzymatic Electrochemistry. *ChemElectroChem* **2025**, *12* (21), No. e202500287.
(10) Bueno, P. R. On the Fundamentals of Quantum Rate Theory and the Long-Range Electron Transport in Respiratory Chains. *Chem. Soc. Rev.* **2024**, *53* (11), 5348−5365.
(11) Dumont, R.; Dowdell, J.; Song, J.; Li, J.; Wang, S.; Kang, W.; Li, B. Control of Charge Transport in Electronically Active Systems towards Integrated Biomolecular Circuits (IbC). *J. Mater. Chem. B* **2023**, *11* (35), 8302−8314.
(12) Bagdžiūnas, G.; Ramanavičius, A. Towards Direct Enzyme Wiring: A Theoretical Investigation of Charge Carrier Transfer Mechanisms between Glucose Oxidase and Organic Semiconductors. *Phys. Chem. Chem. Phys.* **2019**, *21* (6), 2968−2976.
(13) Vecelyte, G.; Dudkaitė, V.; Šedo, O.; Zdráhal, Z.; Bagdžiūnas, G. Tyrosine-Specific Bioconjugation Allowing Hole Hopping along Aromatic Chains of Glucose Oxidase. *Mater. Horiz.* **2025**, *12* (16), 6301−6309.
(14) Damala, P.; Tiuftiakov, N. Yu.; Bakker, E. Avoiding Potential Pitfalls in Designing Wired Glucose Biosensors. *ACS Sens.* **2024**, *9* (1), 2−8.
(15) Dudkaite, V.; Bagdziunas, G. Functionalization of Glucose Oxidase in Organic Solvent: Towards Direct Electrical Communication across Enzyme-Electrode Interface. *Biosensors* **2022**, *12* (5), No. 335, DOI: 10.3390/bios12050335.
(16) Tomizawa, M.; Hosaka, R.; Miura, D.; Ikebukuro, K. Wash-Free Electrochemical Biosensor for CpG Methylation Using a Quasi-Direct Electron Transfer Type Enzyme as the Labeling Enzyme. *Biosens. Bioelectron.* **2026**, *295*, No. 118285.
(17) Ikegai, K.; Okuda-Shimazaki, J.; Tran, T. T.; Hatada, M.; Asano, R.; Ikebukuro, K.; Tsugawa, W.; Sode, K. The 2.5th Generation Enzymatic Sensors Based on the Construction of Quasi-Direct Electron Transfer Type NAD(P)-Dependent Dehydrogenases. *Biosens. Bioelectron.* **2024**, *255*, No. 116219.
(18) Jayakumar, K.; Reichhart, T. M. B.; Schulz, C.; Ludwig, R.; Felice, A. K. G.; Leech, D. An Oxygen Insensitive Amperometric Glucose Biosensor Based on An Engineered Cellobiose Dehydrogenase: Direct versus Mediated Electron Transfer Responses. *ChemElectroChem* **2022**, *9* (13), No. e202200418.
(19) Han, M.; Yoon, S.; Lee, J.; Chung, T. D.; Song, W. J. Redirecting Electron Flows in Glutamate Oxidases by Selective Anchoring of Osmium Complexes. *Chem. Sci.* **2025**, *16* (17), 7433−7441.
(20) Krainer, F. W.; Glieder, A. An Updated View on Horseradish Peroxidases: Recombinant Production and Biotechnological Applications. *Appl. Microbiol. Biotechnol.* **2015**, *99* (4), 1611−1625.
(21) Hamid, M.; Khalil-ur-Rehman. Potential Applications of Peroxidases. *Food Chemistry* **2009**, *115*, 1177−1186.
(22) Hnasko, R. M. Bioconjugation of Antibodies to Horseradish Peroxidase (HRP). In *ELISA: Methods and Protocols*; Hnasko, R., Ed.; Springer: New York, NY, 2015 ; pp 43−50 DOI: 10.1007/978-1-4939-2742-5_4.
(23) Kondzior, M.; Grabowska, I. Antibody-Electroactive Probe Conjugates Based Electrochemical Immunosensors. *Sensors* **2020**, *20* (7), No. 2014.
(24) Carolan, N.; Forster, R. J.; Ó'Fágáin, C. Covalent Attachment of Ferrocene to Soybean Peroxidase Glycans: Electron Transfer Mediation to Redox Enzymes. *Bioconjugate Chem.* **2007**, *18* (2), 524−529.
(25) Chaubey, A.; Malhotra, B. D. Mediated Biosensors. *Biosens. Bioelectron.* **2002**, *17* (6), 441−456.
(26) Dudkaite, V.; Bagdziunas, G. Functionalization of Glucose Oxidase in Organic Solvent: towards Direct Electrical Communication across Enzyme-Electrode Interface. *Biosensors* **2022**, *12* (5), No. 335, DOI: 10.3390/bios12050335.
(27) Zhou, Y.; Yin, H.; Meng, X.; Xu, Z.; Fu, Y.; Ai, S. Direct Electrochemistry of Sarcosine Oxidase on Graphene, Chitosan and Silver Nanoparticles Modified Glassy Carbon Electrode and Its Biosensing for Hydrogen Peroxide. *Electrochim. Acta* **2012**, *71*, 294−301.
(28) Santos, S. R.; Maia, G. Direct Charge Transfer to Horseradish Peroxidase Revisited Using a Glassy Carbon Electrode. *Electrochim. Acta* **2012**, *71*, 116−122.
(29) Wilkins, D. K.; Grimshaw, S. B.; Receveur, V.; Dobson, C. M.; Jones, J. A.; Smith, L. J. Hydrodynamic Radii of Native and Denatured Proteins Measured by Pulse Field Gradient NMR Techniques. *Biochemistry* **1999**, *38* (50), 16424−16431.
(30) Jurrus, E.; Engel, D.; Star, K.; Monson, K.; Brandi, J.; Felberg, L. E.; Brookes, D. H.; Wilson, L.; Chen, J.; Liles, K.; Chun, M.; Li, P.; Gohara, D. W.; Dolinsky, T.; Konecny, R.; Koes, D. R.; Nielsen, J. E.; Head-Gordon, T.; Geng, W.; Krasny, R.; Wei, G.-W.; Holst, M. J.; McCammon, J. A.; Baker, N. A. Improvements to the APBS Biomolecular Solvation Software Suite. *Protein Sci.* **2018**, *27* (1), 112−128.
(31) Zhang, Y.; Nakajima, Y.; Kurobe, M.; Nakamura, T.; Himiyama, T.; Nishiya, Y. Structural and Functional Analysis of *Bacillus* Sarcosine Oxidase and Its Activity toward Cyclic Imino Acids. *FEBS Open Bio* **2025**, *15* (11), 1814−1826.
(32) Berglund, G. I.; Carlsson, G. H.; Smith, A. T.; Szöke, H.; Henriksen, A.; Hajdu, J. The Catalytic Pathway of Horseradish Peroxidase at High Resolution. *Nature* **2002**, *417* (6887), 463−468.
(33) Moulahoum, H.; Ghorbanizamani, F. The LOD Paradox: When Lower Isn't Always Better in Biosensor Research and Development. *Biosens. Bioelectron.* **2024**, *264*, No. 116670.
(34) Li, J.; Ma, J.; Zhang, Y.; Zhang, Z.; He, G. An Amperometric Biosensor for the Assay of Sarcosine Based on the Cross Coupled Chemical and Electrochemical Reactions with Practical Applications. *J. Electroanal. Chem.* **2019**, *833*, 568−572.
(35) Kumar, P.; Narwal, V.; Jaiwal, R.; Pundir, C. S. Construction and Application of Amperometric Sarcosine Biosensor Based on SOxNPs/AuE for Determination of Prostate Cancer. *Biosens. Bioelectron.* **2018**, *122*, 140−146.
(36) Rajarathinam, T.; Kwon, M.; Thirumalai, D.; Kim, S.; Lee, S.; Yoon, J.-H.; Paik, H.; Kim, S.; Lee, J.; Ha, H. K.; Chang, S.-C. Polymer-Dispersed Reduced Graphene Oxide Nanosheets and Prussian Blue Modified Biosensor for Amperometric Detection of Sarcosine. *Anal. Chim. Acta* **2021**, *1175*, No. 338749.

Downloaded from pubs.acs.org/acsodf/article-pdf/doi/10.1021/acsomega.6c04756/6907591/2/acsomega.6c04756.pdf by guest on 04 November 2026